

# Probing equilibration with respect to isospin degree of freedom in intermediate energy heavy ion collisions \*

Qingfeng Li<sup>1)</sup>, Zhuxia Li<sup>1,2,3)</sup>

1) *China Institute of Atomic Energy, P. O. Box 275 (18), Beijing 102413, P. R. China*

2) *Center of Theoretical Nuclear Physics, National Laboratory of Lanzhou Heavy Ion Accelerator, Lanzhou 730000, P. R. China*

3) *Institute of Theoretical Physics, Academia Sinica, P. O. Box 2735, Beijing 100080, P. R. China*

## Abstract

We have studied equilibration with respect to isospin degree of freedom in four 96 mass systems  $^{96}\text{Ru} + ^{96}\text{Ru}$ ,  $^{96}\text{Ru} + ^{96}\text{Zr}$ ,  $^{96}\text{Zr} + ^{96}\text{Ru}$ ,  $^{96}\text{Zr} + ^{96}\text{Zr}$  at 100 AMeV and 400 AMeV with isospin dependent QMD. We propose that the neutron-proton differential rapidity distribution is a sensitive probe to the degree of equilibration with respect to the isospin degree of freedom. By analyzing the average  $N/Z$  ratio of emitted nucleons, light charged particles (LCP) and intermediate mass fragments (IMF), it is found that there exist memory effect in multifragmentation process. The average  $N/Z$  ratio of IMF reduces largely as beam energy increases from 100 AMeV to 400 AMeV which may result from the change of the behavior of the isotope distribution of IMF charges. The isotope distribution of IMF charges does also show certain memory effect at 100 AMeV case but not at 400 AMeV case.

---

\*Supported by National Natural Science Foundation of China under Grant No. 19975073, and Science Foundation of Nuclear Industry and the Major State Basic Research Development Program under the contract No. G20000774

The study of whether the equilibrium is reached or not is a prerequisite for the extraction of valid information about the thermodynamical properties of the excited system produced in the reaction. This problem has been studied theoretically and experimentally for many years. But still there is many new problems which need to further study. Especial interest is about the nature of the multifragmentation that is if the multifragmentation is a statistical emission process or the dynamical one [1–5]. To clarify this problem, the FOPI collaboration recently performed a so-called 'mixing experiment' using four mass 96+96 systems  $Ru + Ru$ ,  $Zr + Zr$ ,  $Ru + Zr$ ,  $Zr + Ru$  at 400 AMeV [6,7]. To quantify conveniently the 'degree of mixing', they defined a normalized proton counting by the value of  $Zr + Zr$  and  $Ru + Ru$ ,

$$R_Z = \frac{2 * Z - Z^{Zr} - Z^{Ru}}{Z^{Zr} - Z^{Ru}}. \quad (1)$$

They first measured the proton counting number for  $Ru + Ru$  and  $Zr + Zr$  then they measured  $R_Z$  for asymmetric reaction  $Zr + Ru$ . The results of  $R_Z$  for reaction  $Zr + Ru$  showed that the protons were not emitted from an equilibrium source and the reaction was half transparent [6]. These experimental results told us that the equilibrium was not eventually reached in the reaction. However, this beautiful experiment study has only shown that at beam energy 400 AMeV the protons are emitted by a non-equilibrium source but it still can not answer if multifragmentation is a statistical emission process or dynamical emission one at lower energy.

The aim of this work is to test the non-equilibrium effect by means of isospin degree of freedom relevant probes stimulated by the 'mixing experiments' performed by FOPI collaboration. We will first introduce our model briefly then we study the normalized proton counting  $R_Z$  and other probes such as the proton rapidity distribution, neutron-proton differential rapidity distribution, and the isospin distribution of emitted nucleons, light charged particles and intermediate mass fragments in the same collision systems at 400 AMeV as well as 100 AMeV. And finally a short conclusion will be given.

The Isospin Dependent Quantum Molecular Dynamics (QMD) model [4,8] is used in the calculations. The following modifications in QMD model are introduced: Firstly, the isospin dependent part of the nuclear potential is taken into account in addition to the Coulomb interaction. The symmetry potential energy per nucleon is taken as the following form,

$$V_{sym}(\rho, \delta) = \frac{C_S}{2} \left( \frac{\rho}{\rho_0} \right) \delta^2, \quad (2)$$

where

$$\delta = \frac{\rho_n - \rho_p}{\rho_n + \rho_p}, \quad (3)$$

and  $C_S$  is the strength of symmetry potential energy. In this work it is taken to be 35 MeV and the corresponding symmetry energy is about 29 MeV. Secondly, the isospin dependent binary elastic scattering cross section is used. It is well known that up to hundreds MeV the free elastic proton-neutron cross section is about 2-3 times larger than that of proton-proton (neutron-neutron)'s. Finally, in the treatment of the Pauli blocking, we firstly distinguish protons and neutrons, and then we use the following two criteria:

$$\frac{4\pi}{3} r_{ij}^3 \cdot \frac{4\pi}{3} p_{ij}^3 \geq \frac{h^3}{4}, \quad (4)$$

and

$$P_{block} = 1 - (1 - f_i)(1 - f_j), \quad (5)$$

where  $f_i$  is the distribution function in phase space for particle  $i$  and reads as

$$f_i(\vec{r}, \vec{p}, t) = \frac{1}{\pi \hbar^3} \exp(-(\vec{r} - \vec{r}_i(t))^2 / 2L^2) \exp(-(\vec{p} - \vec{p}_i(t))^2 2L^2 / \hbar^2). \quad (6)$$

Where  $L$  is a parameter which represents the spatial spread of wave packet,  $\vec{r}_i(t)$  and  $\vec{p}_i(t)$  denote the center of the wave packet in coordinate and momentum space respectively. The first condition gives the criterion for the uncertainty relation of the centroids of Gaussian wave packets of two particles. The second one is the probability of the Pauli blocking effect for the scattering of two particles, which is especially useful for collisions of heavy nuclei. The

soft EOS ( $K = 200\text{MeV}$ ) is used in the calculations, the corresponding main parameters are listed in Table 1. The secondary deexcitation on primary hot fragments is not taken into account in the present calculations. It should not change the general conclusion of this work.

We firstly investigate the proton counting for the mixing reactions of four mass  $96 + 96$  systems  $Ru + Ru$ ,  $Zr + Zr$ ,  $Ru + Zr$ ,  $Zr + Ru$  as the same as in the experimental study in ref. [6]. According to the definition of  $R_Z$ ,  $R_Z = 1$  for  $Zr + Zr$ ,  $R_Z = -1$  for  $Ru + Ru$ . For asymmetric reaction  $Ru + Zr$ ,  $Zr + Ru$ , it may be more convenient to express  $R_Z$  as  $R_z = 2R_{mix} - 1$ , for  $Zr + Ru$  and  $R_z = 1 - 2R_{mix}$  for  $Ru + Zr$ , which can be derived from definition (1). Here  $R_{mix}$  is the percentage of the number of protons emitted from projectile.  $R_{mix}$  is proportional to the degree of mixing of projectile and target. It is obvious that if projectile and target is completely mixed then  $R_{mix}$  equals to 0.5 at any rapidity and if the reaction is full transparent  $R_{mix}$  should equal to 1 at projectile rapidity and 0 at target rapidity, respectively. Fig. 1 shows  $R_Z$  as function of rapidity at beam energy 100 AMeV impact parameter  $b = 0fm$  and 400 AMeV  $b = 0fm$  and  $b = 5fm$ . The experimental data (at 400 AMeV) is also given in the figure. From this figure, one can easily find that the absolute  $R_Z$  value goes from zero to about 0.5 for reactions  $Zr + Ru$  and  $Ru + Zr$  at energy 100 AMeV and 400 AMeV  $b = 0fm$ , and about 0.75 for the same reactions at beam energy 400 AMeV,  $b = 5fm$ . Our calculation is in reasonable agreement with experiments data and consequently, the same conclusion concerning the non-equilibrium effect can be drawn for 400 AMeV case. The results for  $b = 0fm$  and  $b = 5fm$  show the non-equilibrium effect strongly depends on the impact parameter. However, the results of  $R_Z$  for 400 AMeV and 100 AMeV at  $b = 0fm$  are undistinguishable and they lead to the same conclusion that the protons are produced in a non-equilibrium source at both 400 AMeV and 100 AMeV. It seems to us that  $R_Z$  is not very sensitive to the energy dependence of the mixing of projectile and target at the energy range studied in this work. We also find that  $R_Z$  is also not sensitive to the symmetry potential, which will be discussed in our another work. In the following we make further investigation in order to find other possible probes which may

provide more clear information for the energy dependence of the degree of equilibrium.

Fig. 1

In Fig. 2 a)-b) we show the rapidity distribution of emitted protons at beam energy 100 AMeV and 400 AMeV. From Fig. 2 a) and b) we can find that the reaction  $^{96}\text{Ru} + ^{96}\text{Ru}$  emits more protons than that of  $^{96}\text{Zr} + ^{96}\text{Zr}$  because of 8 protons difference for two reaction systems. The proton rapidity distribution for  $^{96}\text{Zr} + ^{96}\text{Ru}$  and  $^{96}\text{Ru} + ^{96}\text{Zr}$  is between those of  $\text{Ru} + \text{Ru}$  and  $\text{Zr} + \text{Zr}$ . Differing from the symmetric reaction  $\text{Ru} + \text{Ru}$  and  $\text{Zr} + \text{Zr}$ , the rapidity distribution of emitted protons for  $\text{Ru} + \text{Zr}$  and  $\text{Zr} + \text{Ru}$  is asymmetric and the peaks deviate from  $Y = 0$ . It again means that the protons are emitted from a non-equilibrium source. But again we find it is difficult to give clear energy dependence of the degree of equilibrium reached. As we know that comparing with the most stable isotopes  $^{102}\text{Ru}$  and  $^{90}\text{Zr}$ ,  $^{96}\text{Ru}$  is of 6 neutron deficiency and  $^{96}\text{Zr}$  is of 6 neutron excess. The ratio between proton number and neutron number for  $^{96}\text{Ru}$  and  $^{96}\text{Zr}$  is 0.85 and 0.71, respectively. It would be more desirable to study the rapidity distribution of the isovector density of emitting nucleons for isospin asymmetric nuclear systems. Therefore we introduce the neutron-proton differential rapidity distribution. Fig. 3 a), b) and c) show the neutron-proton differential rapidity distribution for  $^{96}\text{Ru} + ^{96}\text{Ru}$ ,  $^{96}\text{Zr} + ^{96}\text{Zr}$ ,  $^{96}\text{Zr} + ^{96}\text{Ru}$ ,  $^{96}\text{Ru} + ^{96}\text{Zr}$  at a) 100 AMeV,  $b = 0fm$ , b) 400 AMeV,  $b = 0fm$  and c) 400 AMeV,  $b = 5fm$ . First, for all three cases a), b) and c), the centroids of neutron-proton differential rapidity distribution for  $^{96}\text{Ru} + ^{96}\text{Zr}$ ,  $^{96}\text{Zr} + ^{96}\text{Ru}$  are located at the side of Zr (as target or projectile) and strongly deviate from  $Y = 0$ . The centroid of distribution should be at  $Y = 0$  if a system is in equilibrium. The deviation of the centroid of neutron-proton differential rapidity distribution from  $Y = 0$  means there is non-equilibrium effect. The larger the deviation from  $Y = 0$  is the stronger the non-equilibrium effect is. The deviation of the centroid of neutron-proton differential rapidity distribution from  $Y = 0$  for  $b = 5fm$  case is much larger than that for  $b = 0fm$  case. This is of course quite understandable. Further more, one can find that the neutron-proton differential rapidity distribution of symmetric reactions  $^{96}\text{Ru} + ^{96}\text{Ru}$ ,  $^{96}\text{Zr} + ^{96}\text{Zr}$  at 100

AMeV deviates from the Gaussian shape more strongly than that at 400 AMeV. It implies that there exist obvious non-equilibrium effect in the emitting nucleon process. Therefore we can conclude that the neutron-proton differential rapidity distribution is a sensitive probe to explore the energy dependence of the degree of equilibrium for an isospin asymmetric system. We may generalize the neutron-proton differential rapidity distribution by introducing  $t$ - ${}^3\text{He}$  differential rapidity distribution to probe equilibration in isospin asymmetric colliding systems.

Fig. 2 a), b)

Fig. 3 a), b), c)

However, emitted single nucleons can only characterize limited part of the system, therefore we further study the isospin distribution in LCP and IMF in addition to nucleons. In Fig. 4 (I) and (II), we show the average  $N/Z$  ratios in emission of nucleons, LCP and IMF at projectile (a)), central (b)) and target (c)) rapidity region in four systems at 400 AMeV and 100 AMeV,  $b = 0\text{fm}$ , respectively. The projectile rapidity region is defined by  $1.5 \geq Y \geq 0.5$ , the target rapidity region  $-0.5 \geq Y \geq -1.5$  and the central rapidity region  $0.5 \geq Y \geq -0.5$ . The figures firstly tell us a basic feature that the difference between the average  $N/Z$  ratios of emitted nucleons of 4 colliding systems with different isospin asymmetry is much larger than that between the average ratios of LCP and IMF of 4 systems at three rapidity regions, i.e., the more neutron (proton) rich systems emit more neutrons (protons) while the average  $N/Z$  ratios of LCP and IMF for these four systems are relatively close. This behavior is stronger at 100 AMeV case. The experimental measurements at tens AMeV energy region [10] found that the more asymmetric the system is the stronger the system will be breaking up into still more neutron rich (deficient) light fragments while the  $N/Z$  ratio of heavier fragments remains relatively insensitive. Our calculation results show similar tendency, only because of the energy difference, here the  $N/Z$  ratios of emitted nucleons, LCP and IMF are compared instead of comparing the  $N/Z$  ratios for LCP and IMF in [10] where the energy

was relatively low. The second feature is that the average  $N/Z$  ratio of emitted nucleons generally is the largest, and then, that of LCP and the  $N/Z$  ratio of IMF is the smallest in all rapidity region, which implies that the single nucleons are more neutron rich and LCP and IMF are more isospin symmetric.

It is more meaningful to investigate whether the  $N/Z$  ratio of IMF for mixing reaction converges or not as far as the degree of equilibrium is concerned because IMF produce at late stage of reaction [11]. When we attend to the  $N/Z$  ratios at target and projectile rapidity region, we find that not only the  $N/Z$  ratios of emitted nucleons for two mixing reactions  $^{96}\text{Zr} + ^{96}\text{Ru}$  and  $^{96}\text{Ru} + ^{96}\text{Zr}$  but also those of LCP and IMF do not merge each other but they are more close to  $\text{Zr} + \text{Zr}$  or  $\text{Ru} + \text{Ru}$  at respective rapidity region. It means that not only the nucleons but also IMF are not emitted from an completely equilibrium source. Of course, the difference of the average  $N/Z$  ratio of IMF for reactions  $\text{Zr} + \text{Ru}$  and  $\text{Ru} + \text{Zr}$  is weaker than emitted nucleons, which is understandable because IMF produce at later stage. One can further find that the difference of the  $N/Z$  of IMF for  $\text{Zr} + \text{Ru}$  and  $\text{Ru} + \text{Zr}$  at 100 AMeV is larger than that at 400 AMeV. It may also imply the energy dependence of the degree of equilibrium with respect to the isospin degree of freedom. The energy dependence of the degree of equilibrium is because the two-body collisions become more violent as energy increases from 100 AMeV to 400 AMeV.

By comparing Fig. 4 (I) and (II), one can find that the  $N/Z$  ratio decreases as energy increases from 100 AMeV to 400 AMeV for all 4 systems. It would be interesting to study the reason of this behavior. In Fig. 5 we show the yields of the isotopes of the most abundant IMF charges, a) Li, b) Be, c) B for  $\text{Zr} + \text{Zr}$ ,  $\text{Zr} + \text{Ru}$ ,  $\text{Ru} + \text{Zr}$ ,  $\text{Ru} + \text{Ru}$  at 100 AMeV and  $\text{Zr} + \text{Zr}$ ,  $\text{Ru} + \text{Ru}$  at 400 AMeV, respectively. One can easily find that the yields of isotopes of Li, Be, B for 100 AMeV case are about several times larger (for non-neutron rich isotopes) to several tens times larger (for neutron rich isotopes) than those for 400 AMeV case. The curves for isotope distribution of Li, Be, B for 100 AMeV are more flat than those for 400 AMeV and furthermore the most abundant isotopes of Li, Be, B are always those of most stable ones for 100 AMeV case while are always those of the lightest isotopes for 400

AMeV case. Consequently, the average  $N/Z$  of IMF is reduced as energy increases from 100 AMeV to 400 AMeV. The another obvious difference between the isotope distribution of Li, Be, B for 100 AMeV and 400 AMeV case is the dependence of the yields of the neutron rich (deficient) isotopes on the initial system. For 100 AMeV case, the relative yields of the neutron rich (deficient) isotopes depends on the  $N/Z$  ratio of initial system. The initial system with larger  $N/Z$  ratio produces more neutron rich isotopes and vice versa. We notice that for this case (100 AMeV) that the curves of the isotope distribution of Li, Be, B in mixing reactions  $Zr + Ru$  and  $Ru + Zr$  do not merge into one curve but they are close to those of respective reactions  $Zr + Zr$  or  $Ru + Ru$  with the same projectile. It means that there exist certain memory effect at 100 AMeV case. For 400 AMeV case, this memory effect appearing in the isotope distribution of IMF charges disappears.

Fig. 4

Fig. 5

In summary, we have studied the isospin relevant probes: normalized proton counting  $R_Z$ , the proton rapidity distribution, the neutron-proton differential rapidity distribution as well as the  $N/Z$  ratio of single nucleons, LCP, IMF at central, projectile and target rapidity region for four 96 mass systems  $^{96}Ru + ^{96}Ru$ ,  $^{96}Ru + ^{96}Zr$ ,  $^{96}Zr + ^{96}Ru$ ,  $^{96}Zr + ^{96}Zr$  at 100 AMeV and 400 AMeV with isospin dependent QMD. All these probes concerning the single nucleon emission studied in this work show that the emitted nucleons are not from an equilibrium source and there exists obvious non-equilibrium effect. We propose that the neutron-proton differential rapidity distribution is a sensitive probe to the energy dependence of the degree of equilibrium in single nucleon emission in intermediate energy heavy ion collisions. The average  $N/Z$  ratios of IMF in mixing reactions  $^{96}Ru + ^{96}Zr$ ,  $^{96}Zr + ^{96}Ru$  with the same  $N/Z$  and mass do not converge but they are more close to  $Zr + Zr$  or  $Ru + Ru$  at respective rapidity region. The difference of  $N/Z$  ratios of IMF between  $^{96}Ru + ^{96}Zr$ ,  $^{96}Zr + ^{96}Ru$  at 100 AMeV is larger than that at 400 AMeV which shows the energy dependence of the



non-equilibrium effect with respect to isospin degree of freedom. Furthermore, we find the average  $N/Z$  ratios of IMF at projectile and target rapidity region of IMF largely decreases as energy increases from 100 AMeV to 400 AMeV, which may result from the change of the behavior of the isotope distribution of IMF charge from 100 AMeV to 400 AMeV. The analyzing of isotope distribution of IMF charges at projectile rapidity region for four 96 mass systems shows existing of memory effect at 100 AMeV but not at 400 AMeV concerning isospin degree of freedom.

### ACKNOWLEDGMENTS

The author Z. Li thanks the research group for hadron science of Advanced Science Research Center of JAERI for the hospitality, The manuscript is partly finished during her visit there.

## REFERENCES

- [1] R. Nebauer, J. Aichelin, Nucl. Phys. **681**, 353 (2001).
- [2] J.P. Bondorf, A.S. Botvina, A.S. Iljinov, I.N. Mishustin, K. Sneppen. Phys. Rep. **257**, 133 (1995).
- [3] D.H.E Gross and K. Sneppen, Nucl. Phys. **A567**, 417 (1993).
- [4] J. Aichelin, Phys. Rep. **202**, 233 (1991) and references therein.
- [5] P.B. Gossiaux, R. Puri, C. Hartnack, and J. Aichelin, Nucl. Phys. **A619**, 379 (1997).
- [6] F. Rami, et.al., Phys. Rev. Lett. **84**, 1120 (2000),
- [7] W. Reisdorf, FOPI collabration "Multifragmentation" edited by H.Fedmeier, J. Knoll, W. Nörenberg, J. Wambach, 1999.
- [8] C. Hartnack, et.al., Nucl. Phys. **495**, 303 (1989).
- [9] Fan Sheng, Li Zhuxia, Zhao Zhixiang and Ding Dazhao, Eur. Phys. **A4**, 61 (1999).
- [10] S.J. Yennello, M. Veslesky, R. Laforest, et.al., Nucl. Phys. **681**, 317c (2001).
- [11] J.P. Bondorf, A.S. Botvina, I.N. Mishustin, and S.R. Souza, Phys. Rev. Lett. **73**, 628 (1994),

TABLES

TABLE I. Parameters used in calculations

$\alpha(MeV)$	$\beta(MeV)$	$\gamma$	$\rho_0(fm^{-3})$	$K(MeV)$	$L(fm)$	$C_{Yuk}(MeV)$
-356	303	7./6.	0.168	200	2.1	-5.5

## FIGURES

FIG. 1. The proton counting number  $R_z$  as function of rapidity for  $^{96}\text{Ru} + ^{96}\text{Ru}$ ,  $^{96}\text{Ru} + ^{96}\text{Zr}$ ,  $^{96}\text{Zr} + ^{96}\text{Ru}$ ,  $^{96}\text{Zr} + ^{96}\text{Zr}$  at  $E = 100\text{AMeV}$   $b = 0fm$  (a)),  $E = 400\text{AMeV}$   $b = 0fm$  (b)) and  $b = 5fm$  (c)), respectively. The experimental data for 400 AMeV are also given in the figure.

FIG. 2. The rapidity distribution of emitted protons for the same reaction as Fig. 1 a) at 100 AMeV,  $b = 0fm$  and b) at 400 AMeV,  $b = 0fm$ .

FIG. 3. The neutron-proton differential rapidity distribution for the same reactions as Fig. 1 a) at 100 AMeV,  $b = 0fm$  and b) at 400 AMeV,  $b = 0fm$  and c) at 400 AMeV,  $b = 5fm$ .

FIG. 4. (I) The average  $N/Z$  ratio of emitted nucleons, light charged particles and intermediate mass fragments at a) projectile rapidity region, b) central rapidity region, c) target rapidity region for the same reactions as Fig. 1 at  $E = 400\text{AMeV}$ ,  $b = 0fm$ . (II) The same as (I) but at  $E = 100\text{AMeV}$ .

FIG. 5. The isotope distribution of Li, Be, B at projectile region for the same reactions as Fig. 1 at  $E = 100\text{AMeV}$  and  $400\text{AMeV}$ ,  $b = 0fm$ , respectively.

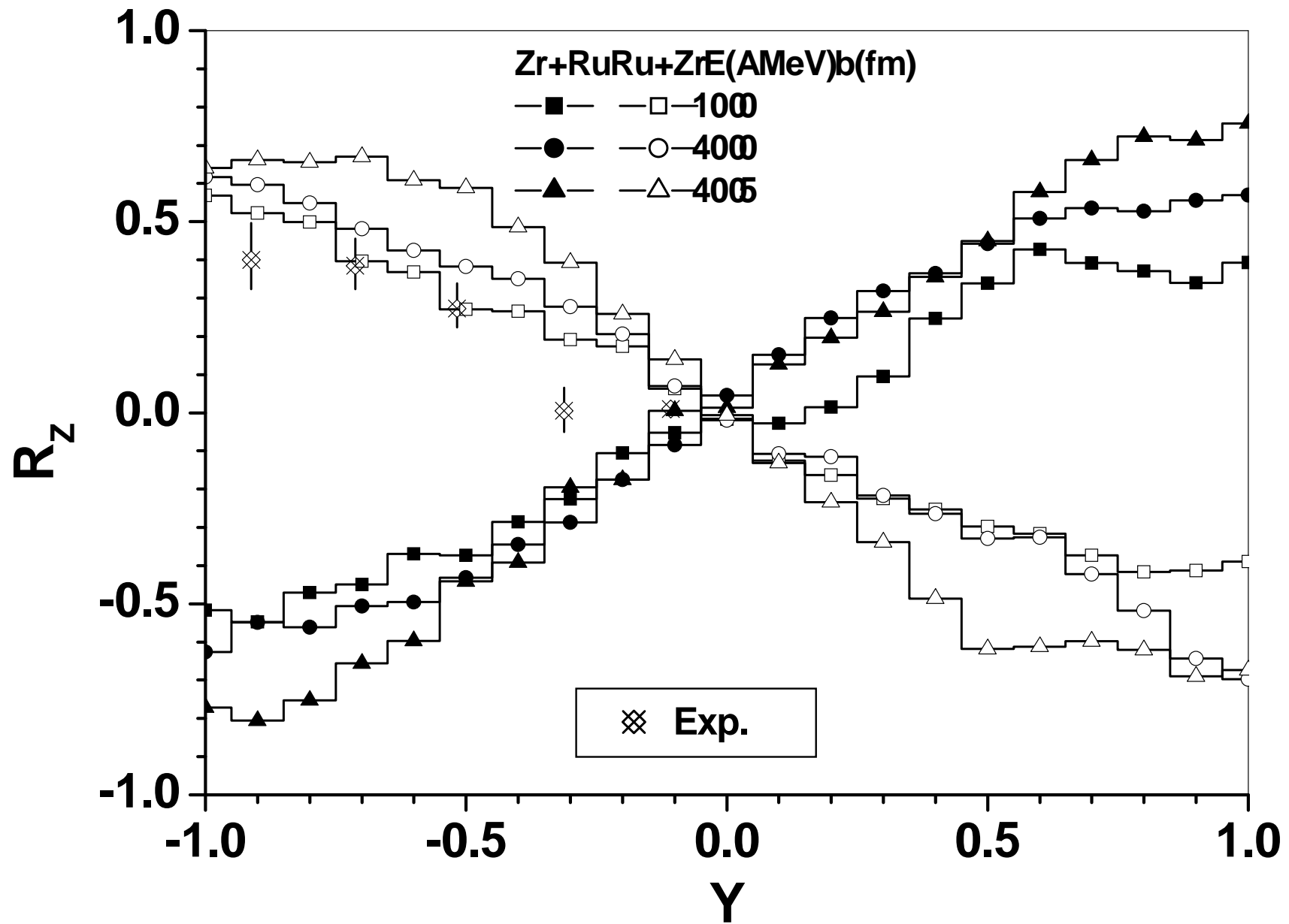


Fig.1

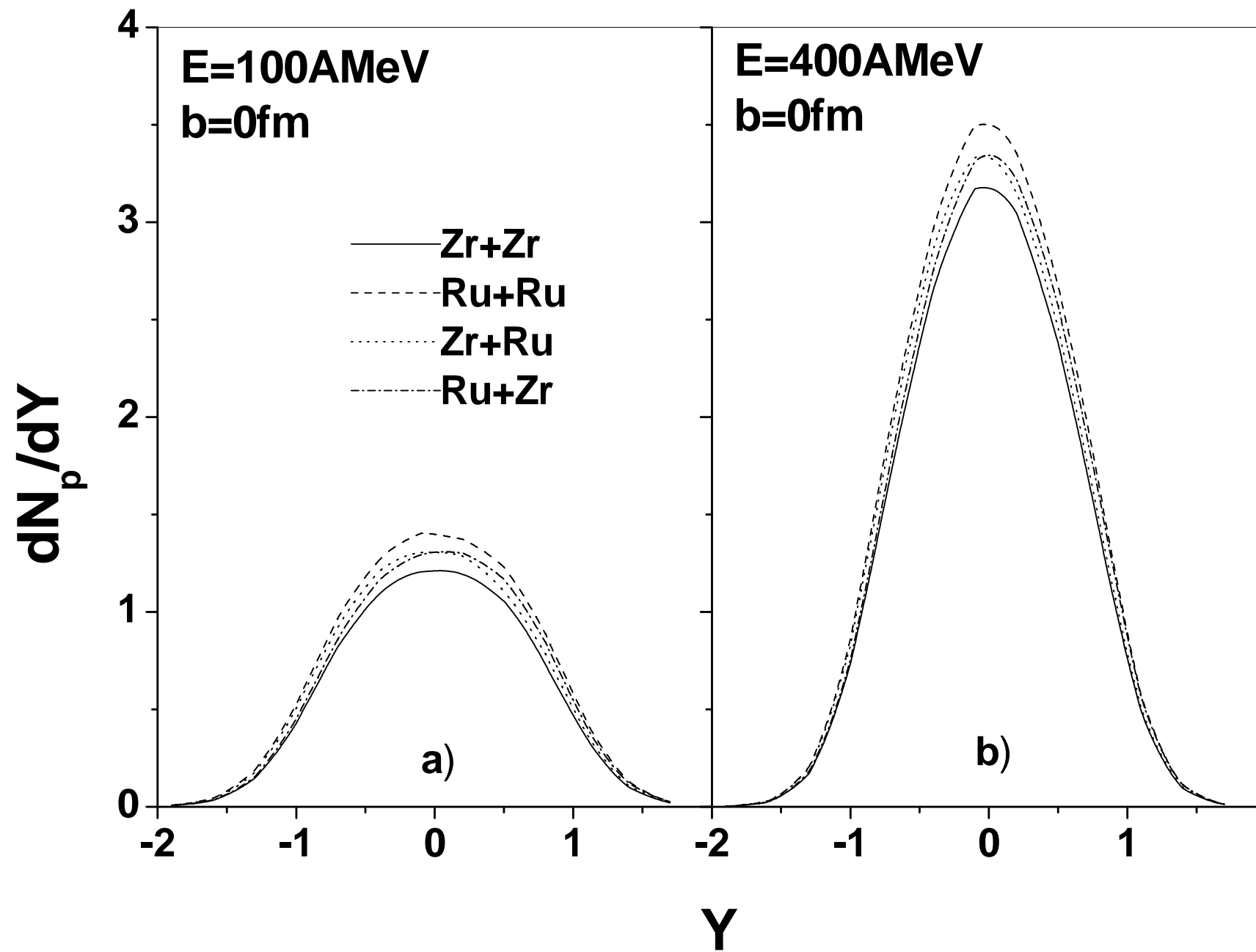


Fig.2

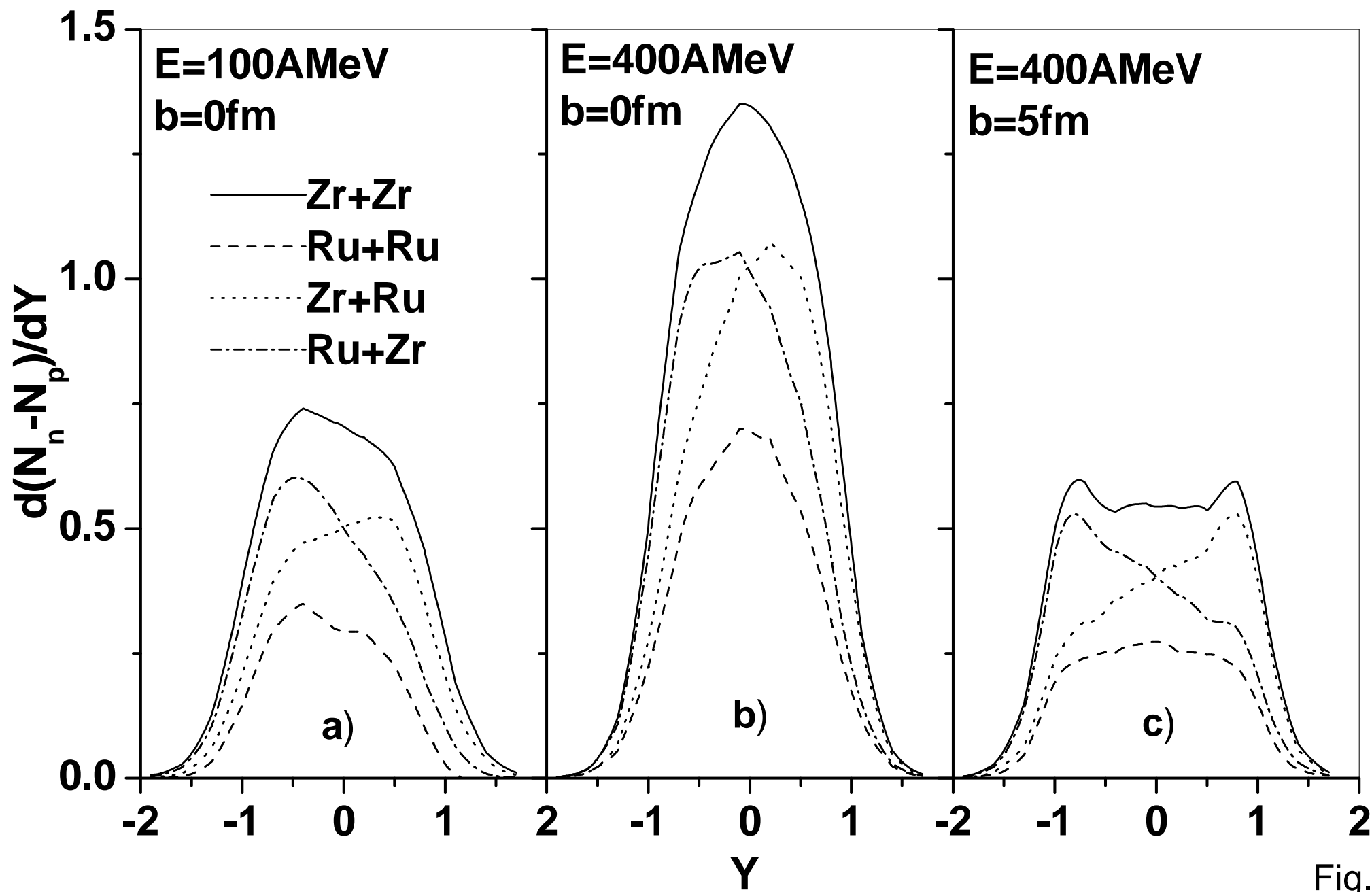
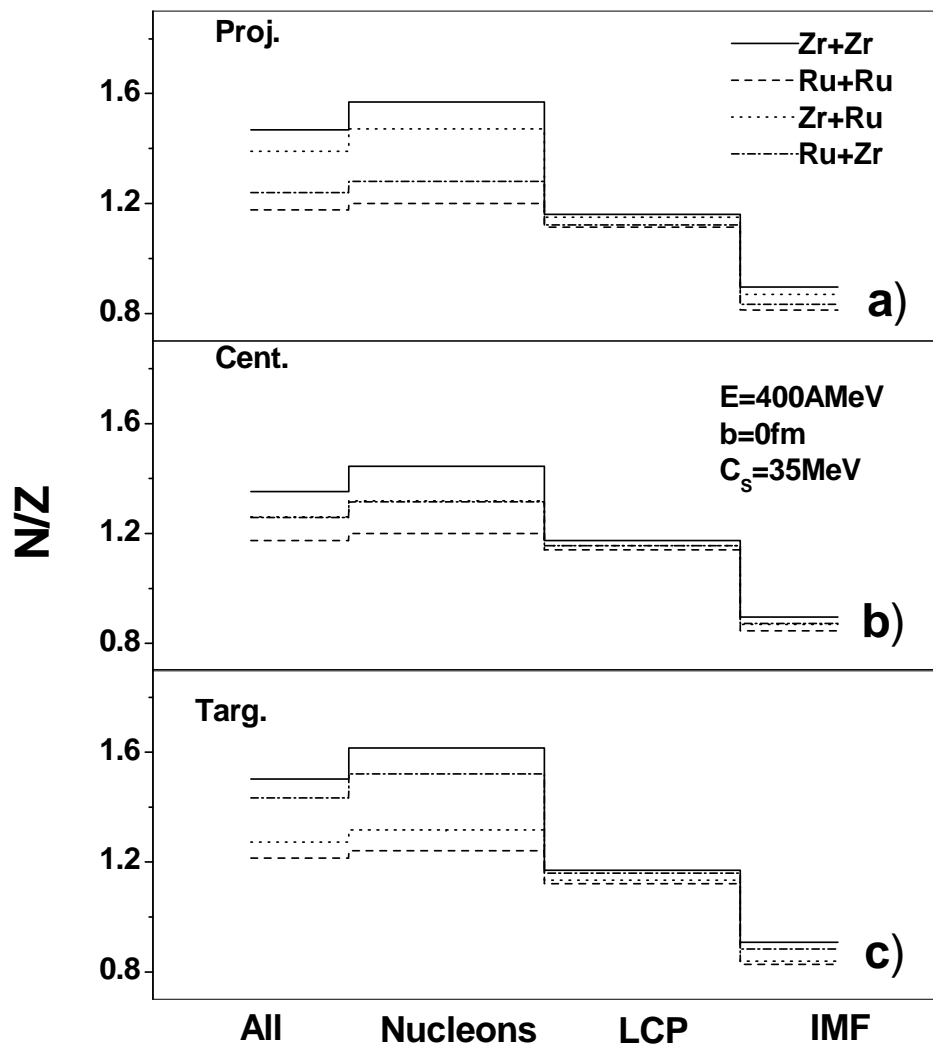


Fig.3

(I)



(II)

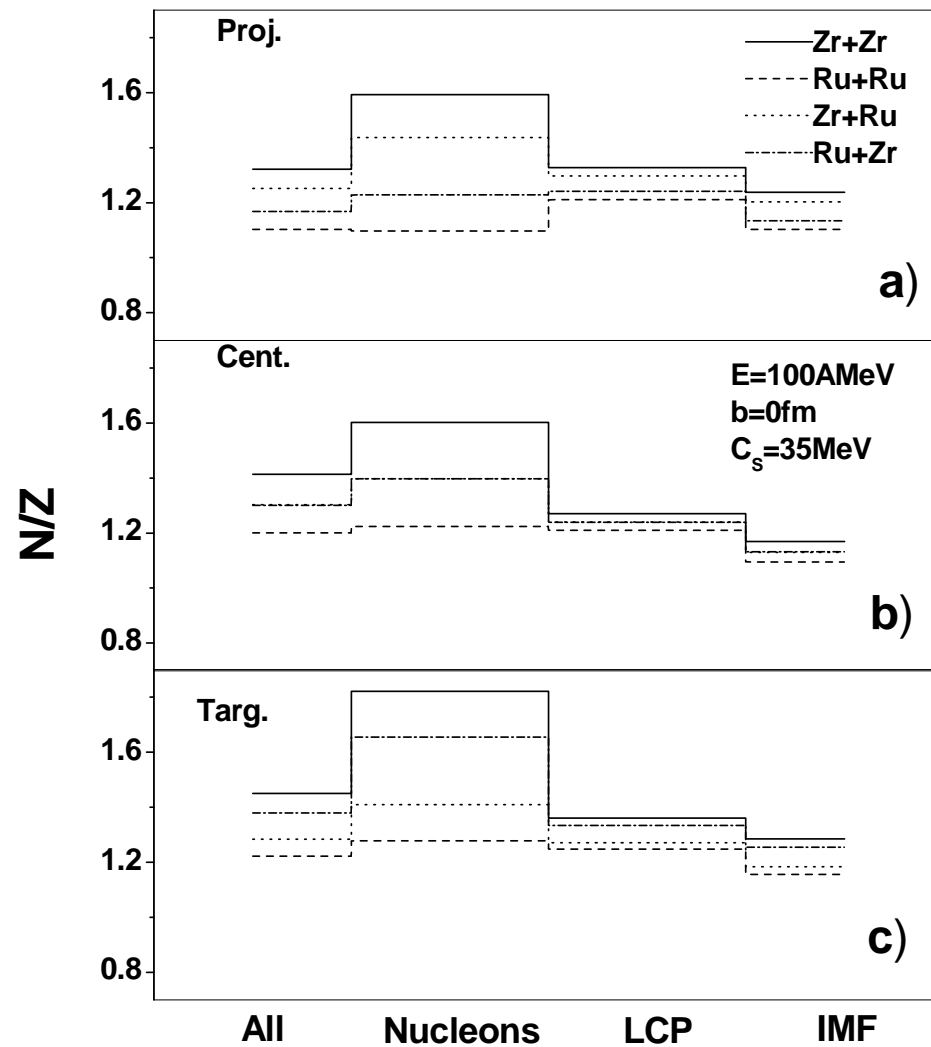


Fig.4



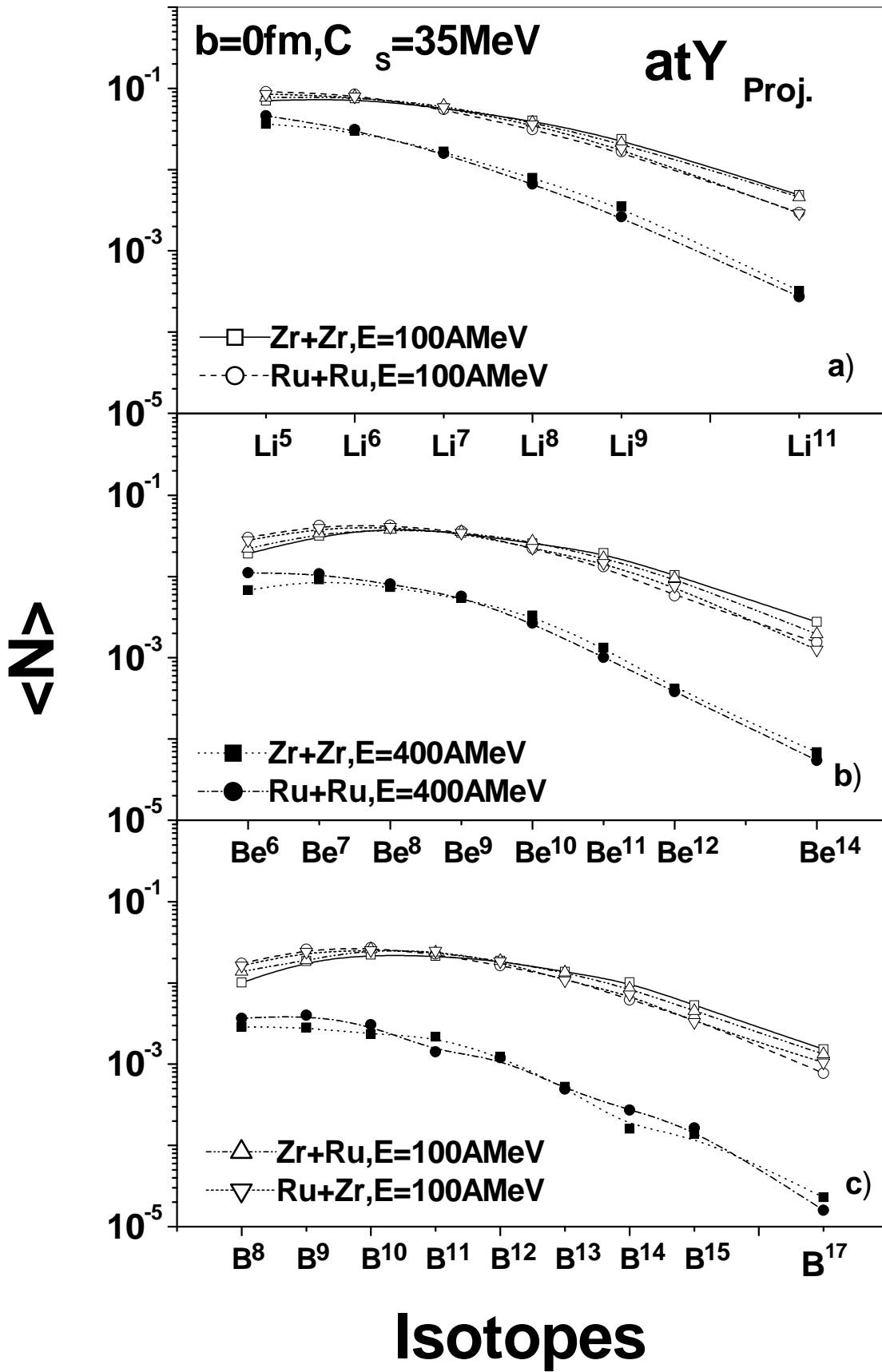


Fig.5